Journal of Physics and Chemistry of Solids 137 (2020) 109219

Contents lists available at ScienceDirect

Journal of Physics and Chemistry of Solids

journal homepage: http://www.elsevier.com/locate/jpcs

New candidate to reach Shockley–Queisser limit: The DFT study of orthorhombic silicon allotrope Si(oP32)

A.S. Oreshonkov [a,b], E.M. Roginskii [c], V.V. Atuchin [d,e,f,*]

[a] Laboratory of Molecular Spectroscopy, Kirensky Institute of Physics Federal Research Center KSC SB RAS, Krasnoyarsk, 660036, Russia
[b] Siberian Federal University, Krasnoyarsk, 660041, Russia
[c] Laboratory of Spectroscopy of Solid State, Ioffe Institute, St. Petersburg, 194021, Russia
[d] Laboratory of Optical Materials and Structures, Institute of Semiconductor Physics, SB RAS, Novosibirsk, 630090, Russia
[e] Functional Electronics Laboratory, Tomsk State University, Tomsk, 634050, Russia
[f] Research and Development Department, Kemerovo State University, Kemerovom, 650000, Russia

ARTICLE INFO

Keywords:
Silicon
Allotrope
Shockley–Queisser limit
DFT
Phonon

ABSTRACT

In the present study, the unit cell parameters and atomic coordinates are predicted for the *Pbcm* orthorhombic structure of Si(oP32) modification. This new allotrope of silicon is mechanically stable and stable with respect to the phonon states. The electronic structure of Si(oP32) is calculated for LDA and HSE06 optimized structures. The band gap value $E_g = 1.361$ eV predicted for Si(oP32) is extremely close to the Shockley–Queisser limit and it indicates that the Si(oP32) modification is a promising material for efficient solar cells. The frequencies of Raman and Infrared active vibrations is calculated for allotrope Si(oP32).

1. Introduction

The diamond-like cubic silicon (Fig. 1) is a semiconductor with the indirect band gap equal to 1.12 eV [1,2]. This elemental material is abundant in nature and, due to its appropriate combination of structural, chemical, mechanical and electronic properties, is widely used in modern electronics, solar cells and chemical industry. Commonly, only the Si allotropes with amorphous and diamond-like structures are widely known as stable at ambient conditions. In the recent decades, the search for new allotropes of Si has attracted considerable attention because most of chemical and physical properties depend on the crystal structure, and it is reasonably expected that new crystal structures might result in novel properties. As a result, many new thermodynamically stable silicon structures were predicted and their properties were theoretically observed [3–11] including the cases when the common tetragonal coordination of Si atoms transform into other forms [3,4,8]. Besides theoretical investigations, the experimental studies were implemented with the use of different preparation routes and several Si allotropes were synthesized to observe their structural and physical characteristics [12–14].

Recently, new germanium allotrope Ge (oP32) with the structure in space group *Pbcm* has been synthesized by the mild-oxidation/delithiation of Li_7Ge_{12} in ionic liquids [15]. The powder and single crystal products were obtained by the reaction at 135-145 °C for several days. It is particularly interesting that Ge (oP32) crystals are stable in ambient conditions. The allotrope has as low direct optical band gap as $E_g = 0.33$ eV and is stable up to 363 °C. Thus, the transformation from the diamond-like to orthorhombic structure results in a drastic band gap energy variation. As for silicon, to the best of our knowledge, the related allotrope Si(oP32) has not been considered up to now and its stability and properties remain unknown. Hence, the present study is aimed at the *ab initio* calculations to evaluate the structure and physical properties of silicon allotrope Si(oP32) isostructural to orthorhombic Ge (oP32).

2. Calculations

All the structural optimization, energy and vibrational calculations were carried out by the CASTEP code using the density-functional theory [16]. The structure of orthorhombic Ge (oP32) with the *Pbcm* space group was taken as the initial basis and the germanium atoms were replaced by silicon ones [15]. This structure was fully optimized using the local density approximation (LDA) provided by the Perdew and Zunger [17] parameterization of the numerical results of Ceperley and Alder (CA-PZ) [18] and using the nonlocal exchange-correlation HSE06 functional [19].

* Corresponding author. Institute of Semiconductor Physics, Novosibirsk, 630090, Russia.
E-mail address: atuchin@isp.nsc.ru (V.V. Atuchin).

https://doi.org/10.1016/j.jpcs.2019.109219
Received 27 August 2019; Received in revised form 24 September 2019; Accepted 1 October 2019
Available online 1 October 2019

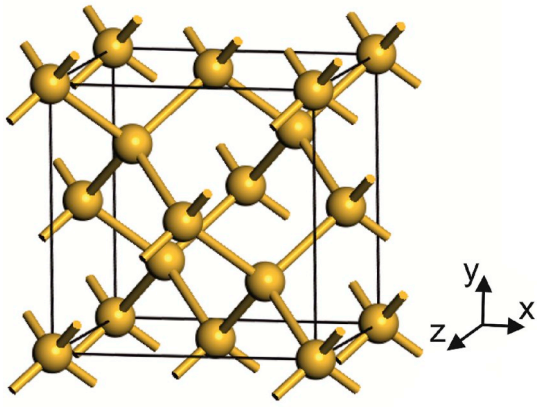

Fig. 1. Crystallographic cell of cubic silicon.

The calculations of both cubic diamond-like and orthorhombic *Pbcm* structures were performed using the norm-conserving pseudopotential with $3s^2$ $3p^2$ electrons for Si atoms treated as valence ones. The self-consistent field (SCF) procedure was used with a convergence threshold of $5.0 \cdot 10^{-8}$ eV/atom. The total energy was corrected for the finite basis set with 3 cut-off energies. The geometry optimizations were performed at the convergence threshold of 0.001 eV $Å^{-1}$ on the max force, 0.01 GPa - on the max stress. The energy cutoff was set to be 900 eV, and the Brillouin zone (BZ) was sampled by $4 \times 3 \times 4$ and $6 \times 6 \times 6$ k-points using the Monkhorst–Pack scheme [20] for orthorhombic and cubic structures, respectively. The electronic band structure was calculated within the hybrid functional HSE06 method [16] as for the structure obtained after the geometry optimization, using HSE06 as for the LDA relaxed structure. The phonon spectra at the Γ-point of the BZ and Raman tensor components were calculated within the density functional perturbation theory and the finite displacement method [21, 22] based on the crystal system type. The Raman spectra were simulated by the Lorentzian distribution with a fixed HWHM equal to 2 cm^{-1}. The dispersion of phonon branches along high symmetry directions of the Brillouin zone was calculated using the linear response method [23].

Quasiparticle *GW* calculations [24] were performed using the ABINIT code [25,26]. The one-shot G_0W_0 quasiparticle energies were computed using the Kohn-Sham eigenstates and eigenvalues calculated within the LDA approximation as the initial solution of non-interacting Hamiltonian. The inverse dielectric matrix $\epsilon^{-1}_{GG'}(q, \omega)$ was calculated by the random phase approximation (RPA) using 192 unoccupied bands. The dynamic screening was calculated using the contour deformation method [27]. The wavefunctions with maximal kinetic energy 35 Ha were used in the calculations. The corrections to Kohn-Sham energies were calculated as $\sum -E_{xc}$ operator diagonal matrix elements, where is self-energy operator, E_{xc} stands for exchange-correlation energy operator, G is Green function, while $W = \epsilon^{-1}v$ determines screening Coulomb interaction operator. The components of wavefunction with energies below 28 Ha for both exchange and correlation parts were used to calculate $\sum$.

3. Results and discussion

The optimized crystal structure of Si(oP32) is shown in Fig. 2 and the obtained crystallographic data are summarized in Table 1. The difference between the calculated unit cell parameters using LDA and HSE06 does not exceed 0.016 Å. The obtained fractional coordinates differ only in the third decimal place.

The mandatory part of mechanical stability of a crystal lattice is the calculations of elastic constants and elastic moduli [28,29]. The elastic behavior of a lattice is described by the second-order elastic constant matrix C_{ij} [30]. The calculated stiffness matrix C_{ij} of orthorhombic *Pbcm*

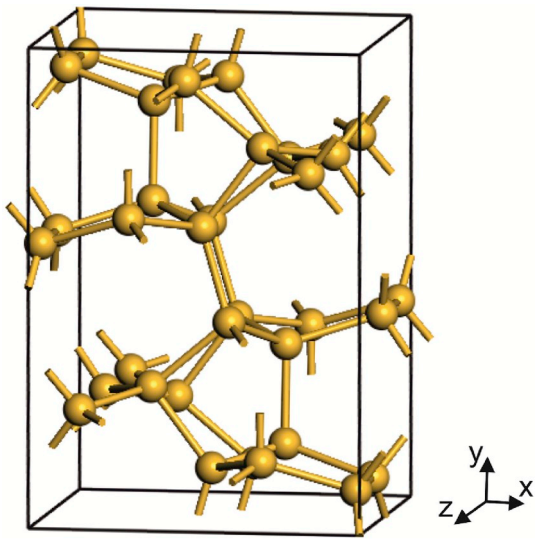

Fig. 2. Crystallographic cell of predicted silicon allotrope Si(oP32).

Table 1
The calculated structural parameters and atomic positions of Si(oP32), as obtained by LDA and HSE06 (shown in parentheses).

Unit cell parameters				
	a, Å	*b*, Å	*c*, Å	
	7.777625 (7.785639)	11.194104 (11.186565)	7.387129 (7.402904)	
Atom	Wyckoff site	Fractional atomic coordinates		
Si1	4d	0.56517 (0.56592)	0.08464 (0.08406)	0.25000 (0.25000)
Si2	4d	0.33135 (0.33106)	0.22142 (0.22017)	0.25000 (0.25000)
Si3	4d	0.48543 (0.48599)	−0.11273 (-0.11346)	0.25000 (0.25000)
Si4	8e	−0.02380 (−0.02378)	0.41322 (0.41340)	0.08613 (0.08639)
Si5	4c	0.15389 (0.15405)	0.25000 (0.25000)	0.00000 (0.00000)
Si6	8e	0.69943 (0.69939)	0.14703 (0.14682)	−0.01212 (-0.01221)

silicon is presented below.

$$C_{ij} = \begin{pmatrix} 146.07 & 45.46 & 51.31 & & & \\ 45.46 & 154.12 & 39.23 & & & \\ 51.31 & 39.23 & 181.75 & & & \\ & & & 44.18 & & \\ & & & & 55.08 & \\ & & & & & 45.76 \end{pmatrix}$$

The *necessary* and *sufficient* Born criteria for an orthorhombic system stability [30] are $C_{11} > 0$, $C_{11}C_{22} > C_{12}^2$, $C_{11}C_{22}C_{33} + 2C_{12}C_{13}C_{23} - C_{11}C_{23}^2 - C_{22}C_{13}^2 - C_{33}C_{12}^2 > 0$, $C_{44} > 0$, $C_{55} > 0$, $C_{66} > 0$. All the above conditions are satisfied for the predicted orthorhombic structure. Thus, the predicted structure of Si(oP32) allotrope is stable with respect to elastic properties. The calculated bulk modulus (B) value is found to be equal to 83.19 GPa. The results obtained in this work for cubic silicon: $B = 98.00$ GPa and $C_{11} = 163.97$ GPa, $C_{12} = 65.02$ GPa, $C_{44} = 77.39$ GPa are in accordance with experimental data: $B = 98$ GPa [31] and $C_{11} = 166$ GPa, $C_{12} = 64$ GPa, $C_{44} = 79.6$ GPa [32].

The electronic band structure calculations were performed for the LDA and HSE06 relaxed structures of orthorhombic *Pbcm* and cubic silicon allotropes. As expected, the strong the band gap value underestimation is found in the local density approximation for the cubic phase. Thus, one may assume that LDA fails to threat the electronic structure of

crystalline Si. On the contrary, the good agreement is found in case of geometry optimization using the HSE06 method followed by the electronic structure calculations using HSE06 also. The calculated E^{i}_{g} value for cubic silicon is in excellent agreement with the experimental one (1.12 eV [1,2]) obtained using the hybrid functional HSE06 method for the structure optimized by the local density approximation. This fact could be used as a good validation of the methods, and, hence, predicted values could be used as a reference for the orthorhombic Si(oP32) allotrope. The calculated data obtained with different approaches are shown in Table 2.

The electronic band structure of Si(oP32) calculated by the hybrid functional HSE06 method for the LDA relaxed structure is plotted in Fig. 3. For the energy band calculations, the high-symmetry points of the BZ are selected as Γ–X–S–Y–Γ–Z–U–R–T–Z. The coordinates of the special points of the Brillouin zone are: Γ (0,0,0), X (0.5,0,0), S (0.5,0.5,0), Y (0,0.5,0), Z (0,0,0.5), U (0.5,0,0.5), R (0.5,0.5,0.5), T (0,0.5,0.5). It is found that the valence band (VBM) top is well localized in the vicinity of the Γ-point in the center of the Brillouin zone. The conduction band (CBM) bottom is located at X-point (0.5, 0, 0). The band gap value for the indirect electronic transitions calculated within the hybrid functional HSE06 approach is equal to $E^{i}_{g} = 1.361$ eV. It is noteworthy to mention that the predicted Si(oP32) band gap value is very close to the theoretical value of Shockley–Queisser limit (1.34 eV) [33,34]. Respectively, the Si(oP32) silicon modification seems to be a promising material for solar cells. The direct band gap is located at the Y-point of the Brillouin zone and the calculated band gap value is $E^{d}_{g} = 1.402$ eV. The results of quasi-particle G_0W_0 approximation are in agreement with the result of hybrid HSE06, and the difference between direct and indirect band gap values is insignificant, too (0.045 eV). However, there is a slight divergence in the band gap values of G_0W_0 approximation ($E^{i}_{g} = 1.127$ eV), with respect to HSE06 calculations ($E^{i}_{g} = 1.362$ eV), which is probably due to the fact that G_0W_0 was performed as "one-shot" calculations, while the calculations with the hybrid functional HSE06 approach were made as self-consisted. Thus, as a result of the electronic band structure analysis, we can conclude that Si(oP32) is a semiconductor material with indirect band gap $E^{i}_{g} = 1.362$ eV. The difference between direct and indirect band gaps is negligible.

The total and partial densities of states of the Si(oP32) silicon allotrope structure obtained with the LDA method are shown in Fig. 4. As a result of the curve analysis, one can find that the VBM and CBM are constructed mostly by the p-electrons of Si atoms, and s-electrons play a secondary role in the CBM formation. It also should be noted that the main contribution of p-electrons appears at the upper portion of valence band, while at the lower portion the contribution of s-electrons becomes more dominant. Such characteristic is similar to silicon carbides and nitrides [35–38].

The mechanical representation for the predicted Si(oP32) allotrope phase of Si (*Pbcm*) at the Brillouin zone center is $\Gamma_{vibr} = 13A_g+10A_u+14B_{1g}+11B_{1u}+11B_{2g}+14B_{2u}+10B_{3g}+13B_{3u}$ [39] where the Raman active modes are $\Gamma_{Raman} = 13A_g+14B_{1g}+11B_{2g}+10B_{3g}$, and the Infrared active modes are $\Gamma_{Infrared} = 10B_{1u}+13B_{2u}+12B_{3u}$. The acoustic modes are $\Gamma_{Acoustic} = B_{1u}+B_{2u}+B_{3u}$. Thus, the Raman spectra of *Pbcm* silicon allotrope contain much more bands than that of cubic silicon. Cubic silicon has only one BZ center optical phonon mode active in the Raman spectrum at 522 cm^{-1} [40].

Table 2
Calculated indirect band gap values (in eV) for cubic and orthorhombic *Pbcm* silicon allotropes.

	Cubic			Orthorhombic *Pbcm*		
Functional for geom. opt.	LDA	LDA	HSE06	LDA	LDA	HSE06
Functional for band str. calc.	LDA	HSE06	HSE06	LDA	HSE06	HSE06
E^{i}_{g} (eV)	0.479	1.113	1.078	0.695	1.361	1.383

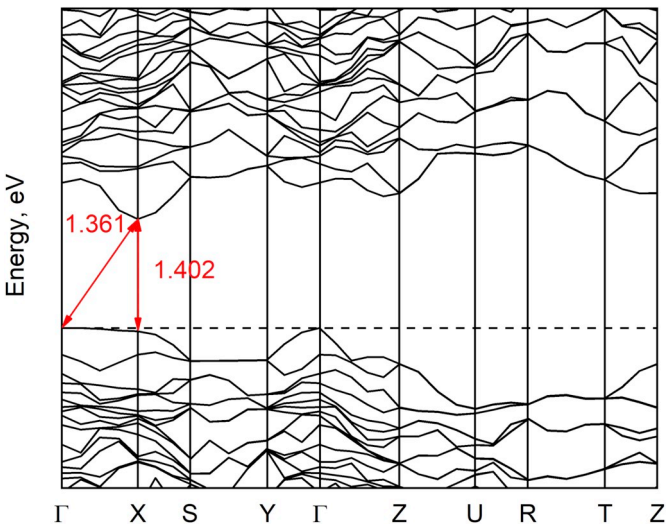

Fig. 3. Electronic band structure of Si(oP32) silicon calculated with the use of HSE06.

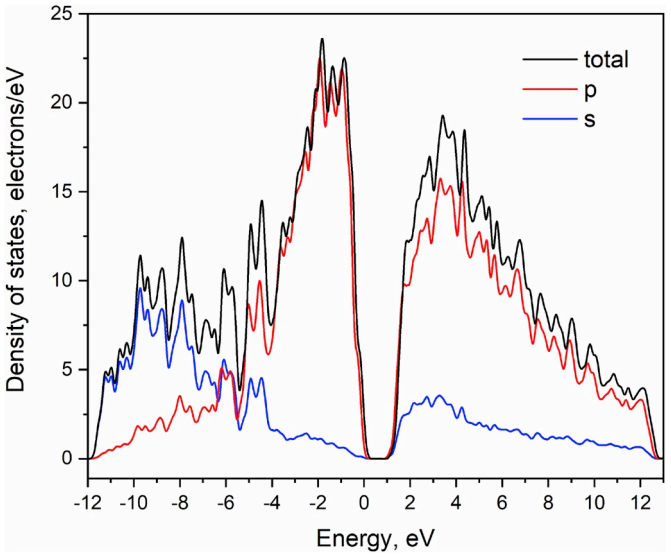

Fig. 4. Total and partial density of states of Si(oP32).

The calculated Raman spectrum of Si(oP32) allotrope is shown in Fig. 5. The spectral line with the highest wavenumber value (533.6 cm^{-1}) is related to the stretching vibration of the shortest bond in the structure (Si1–Si3, see Fig. 6a) and, according to the calculation data, the stretching-like vibrations of different Si–Si pairs are located in the rage of 463–533 cm^{-1}. The various stretching-like and bending-like vibrations of structural units (Fig. 6b) are located in the range of 323–457 cm^{-1}. The weak band at 291.5 cm^{-1}, the most intensive band in the calculated Raman spectrum at 278.1 cm^{-1} and a very weak band at 196.1 cm^{-1} are related to the stretching of the structure as a whole, as shown in Fig. 6c, 6d and 6e correspondingly. The intense line at 129.0 cm^{-1} is a vibration of Si chains, as shown in Fig. 6f.

It is worth noting that the orthorhombic Si(oP32) modification has the IR-active phonons, opposite to cubic silicon. The dynamical properties calculation was carried out and the simulated wavenumbers of Raman and Infrared active modes are listed in Table 3. The calculated phonon dispersion of Si(oP32) structure is shown in Fig. 7. There are no phonon branches with imaginary frequencies, and, hence, the predicted structure should be stable with respect to phonon states.

Earlier, other orthorhombic allotrope of silicon with the structure in

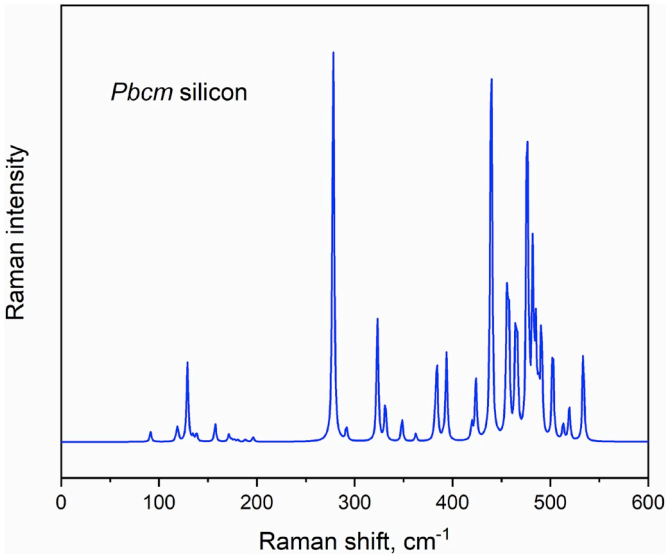

Fig. 5. Calculated Raman spectrum of Si(oP32).

space group *Cmcm* was investigated [14]. In Fig. 8, the energy of the relaxed geometries of cubic and orthorhombic *Pbcm* and *Cmcm* structures as a function of volume per formula unit is shown.

It is clearly seen that the phase transition from cubic to orthorhombic structures with *Cmcm* and *Pbcm* spase groups may occur in the case of increasing the volume per formula unit of cubic silicon. These curves intersection points relate to the ~18.2 and ~23.8% increase of the cubic silicon cell volume. As a possible way of such structure expansion, an intercalation of neutral atoms into the cubic silicone structure may be considered. Herewith, the cubic structure still remains to be stable, with respect to elastic stability conditions and phonon states. Thus, such possible phase transitions should be of the first order type. As evident in Fig. 8, the intersection of the energy per volume curves for *Cmcm* and *Pbcm* phases exist and, thus, the structural transformation is possible from Si_{24} to the Si(oP32) allotrope. Si_{24} (orthorhombic *Cmcm*) silicon was experimentally obtained as a result of thermal 'degassing' of Na_4Si_{24} at 400 K under dynamic vacuum [14]. Ge (oP32) (orthorhombic *Pbcm*) germanium was experimentally prepared by the treatment of Li_7Ge_{12} in ionic liquids [15]. The processes appropriate for the Li intercalation into cubic silicon are well known and, supposedly, they could be developed to reach the Li_7Si_{12} phase [41–44]. Thus, it may be suggested that

Table 3
The calculated vibrational wavenumber values (cm^{-1}) of Si(oP32) allotrope.

№	Raman				Infrared			
	A_g	B_{1g}	B_{2g}	B_{3g}	A_u	B_{1u}	B_{2u}	B_{3u}
1	533.6	519.3	502.4	513.0	501.4	497.2	526.3	515.6
2	490.7	481.4	485.0	487.8	477.0	482.9	486.3	482.2
3	481.9	476.2	478.3	469.2	463.3	474.2	479.0	481.3
4	457.4	464.4	466.2	463.1	451.7	413.9	434.7	465.6
5	455.4	446.6	390.4	419.7	367.2	382.9	415.7	456.0
6	439.5	423.8	348.3	362.5	315.4	185.6	367.5	374.8
7	393.7	382.0	188.4	291.5	178.3	169.2	360.1	339.4
8	383.9	331.2	177.2	176.7	170.5	153.2	320.0	322.4
9	323.2	277.2	138.2	157.4	138.0	130.6	298.2	297.9
10	278.1	196.1	119.0	117.4	110.0	115.8	159.2	253.5
11	171.3	180.6	95.9				150.2	173.3
12	129.0	174.0					135.2	167.4
13	91.3	164.6					119.5	
14		134.7						

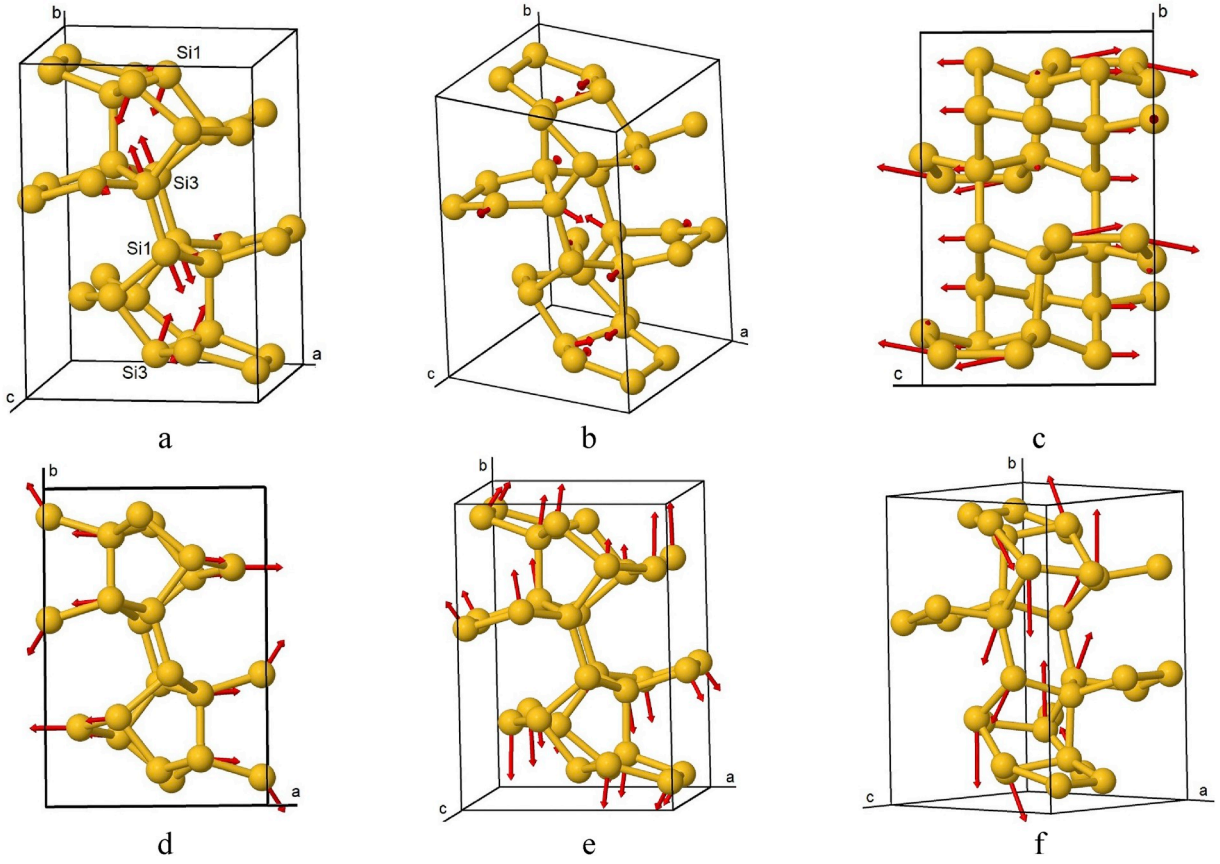

Fig. 6. Atomic displacements contributing to the Raman-active vibrational modes of Si(oP32) allotrope with frequencies 533.6 cm^{-1} (a), 446.7 cm^{-1} (b), 291.5 cm^{-1} (c), 278.1 cm^{-1} (d), 196.1 cm^{-1} (e) and 129.0 cm^{-1} (f).

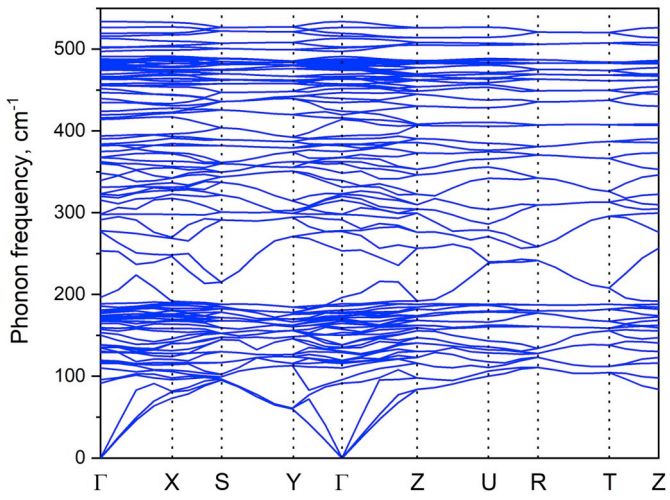

Fig. 7. Calculated phonon dispersion curves of the Si(oP32) allotrope of silicon.

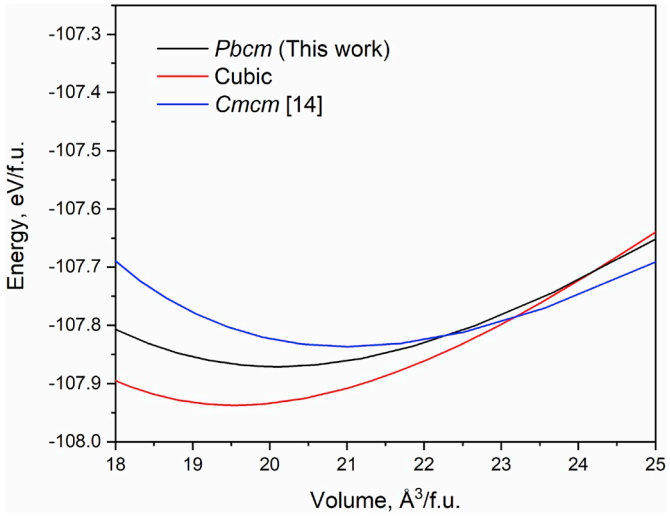

Fig. 8. Total energy per formula unit (f.u.) as a function of the volume per f.u. for cubic and orthorhombic structures of silicon.

similar chemical reactions can also be designed for the formation of Si (oP32) modification. In terms of the total energy minimum, from results of our research follows that the total energy per formula unit for the Si (oP32) structure of orthorhombic silicon predicted in this work is lower than the one for *Cmcm* silicon. Thus, it can be reasonably assumed that the *Pbcm* phase is preferable than the *Cmcm* phase at ambient conditions.

4. Conclusions

In the present study, the unit cell parameters and atomic coordinates were predicted for a new anisotropic modification Si(oP32) of silicon. The Si(oP32) allotrope structure is similar to that of earlier synthesized germanium allotrope Ge (oP32). Respectively, because of chemical and structural similarities, the existence of continuous series of solid solutions Si(oP32)-Ge (oP32) can be assumed. The band gap value $E_g = 1.361$ eV predicted for Si(oP32) is very close to the Shockley–Queisser limit and it indicates that the silicon modification is a promising material for efficient solar cells. Thus, this is the time for the experimental synthesis of Si(oP32) allotrope and detailed exploration of its properties.

Declaration of competing interest

There are no conflicts of interest.

Acknowledgements

The authors are grateful for the support from RFBR, according to the research projects 18-03-00750 and 18-32-20011. The computations were performed using the facilities of the Computational Center of the Research Park of St. Petersburg State University. This study was also supported by the Russian Science Foundation (project 19-42-02003, in part of conceptualization).

References

[1] Y. Okada, Y. Tokumaru, Precise determination of lattice parameter and thermal expansion coefficient of silicon between 300 and 1500 K, J. Appl. Phys. 56 (2) (1984) 314–320.
[2] A.G. Cullis, L.T. Canham, P.D. Calcott, The structural and luminescence properties of porous silicon, J. Appl. Phys. 82 (3) (1997) 909–965.
[3] K. Takeda, K. Shiraishi, Theoretical possibility of stage corrugation in Si and Ge analogs of graphite, Phys. Rev. B 50 (20) (1994) 14916–14922.
[4] G.G. Guzmán-Verri, L.C. Lew Yan Voon, Electronic structure of silicon-based nanostructures, Phys. Rev. B 76 (7) (2007), 075131.
[5] Q. Wang, B. Xu, J. Sun, H. Liu, Z. Zhao, D. Yu, C. Fan, J. He, Direct band gap silicon allotropes, J. Am. Chem. Soc. 136 (28) (2014) 9826–9829.
[6] A. Mujica, C.J. Pickard, R.J. Needs, Low-energy tetrahedral polymorphs of carbon, silicon, and germanium, Phys. Rev. B 91 (2015) 214104.
[7] A.J. Karttunen, D. Usvyat, M. Schütz, L. Maschio, Dispersion interactions in silicon allotropes, Phys. Chem. Chem. Phys. 19 (11) (2017) 7699–7707.
[8] R. Tutchton, C. Marchbanks, Z. Wu, Structural impact on the eigenenergy renormalization for carbon and silicon allotropes and boron nitride polymorphs, Phys. Rev. B 97 (2018) 205104.
[9] P. Zhang, T. Ouyang, C. Tang, C. He, J. Li, C. Zhang, M. Hu, J. Zhong, Thermoelectric properties of four typical silicon allotropes, Model. Simul. Mater. Sci. Eng. 26 (2018), 085006.
[10] M. Hu, Z. Wang, Y. Xu, J. Liang, J. Li, X. Zhu, Fvs-Si48: a direct band gap silicon allotrope, Phys. Chem. Chem. Phys. 20 (2018) 26091–26097.
[11] Q. Fan, R. Niu, W. Zhang, W. Zhang, Y. Ding, S. Yun, *t*-Si_{64}: a novel Si allotrope, ChemPhysChem 20 (1) (2019) 128–133.
[12] P. Vogt, P. De Padova, C. Quaresima, J. Avila, E. Frantzeskakis, M.C. Asensio, A. Resta, B. Ealet, G. Le Lay, Silicene: compelling experimental evidence for graphenelike two-dimensional silicon, Phys. Rev. Lett. 108 (2012) 155501.
[13] B. Haberl, M. Guthrie, S.V. Sinogeikin, G. Shen, J.S. Williams, J.E. Bradby, Thermal evolution of the metastable r8 and bc8 polymorphs of silicon, High Press. Res. 35 (2) (2015) 99–116.
[14] D.Y. Kim, S. Stefanoski, O.O. Kurakevych, T.A. Strobel, Synthesis of an open-framework allotrope of silicon, Nat. Mater. 14 (2015) 169–173.
[15] Z. Tang, A.P. Litvinchuk, M. Gooch, A.M. Guloy, Narrow gap semiconducting germanium allotrope from the oxidation of a layered Zintl phase in ionic liquids, J. Am. Chem. Soc. 140 (22) (2018) 6785–6788.
[16] S.J. Clark, M.D. Segall, C.J. Pickard, P.J. Hasnip, M.J. Probert, K. Refson, M. C. Payne, First principles methods using CASTEP, Z. Kristallogr. 220 (2005) 567–570.
[17] J.P. Perdew, A. Zunger, Self-interaction correction to density-functional approximations for many-electron systems, Phys. Rev. B 23 (1981) 5048–5079.
[18] D.M. Ceperley, D.J. Alder, Ground state of the electron gas by a stochastic method, Phys. Rev. Lett. 45 (1980) 566–569.
[19] A.V. Krukau, O.A. Vydrov, A.F. Izmaylov, G.E. Scuseria, Influence of the exchange screening parameter on the performance of screened hybrid functionals, J. Chem. Phys. 125 (2006) 224106.
[20] H.J. Monkhorst, J.D. Pack, Special points for Brillouin-zone integrations, Phys. Rev. B 13 (1976) 5188–5192.
[21] D. Porezag, M.R. Pederson, Infrared intensities and Raman-scattering activities within density-functional theory, Phys. Rev. B 54 (11) (1996) 7830–7836.
[22] K. Refson, P.R. Tulip, S.J. Clark, Variational density-functional perturbation theory for dielectrics and lattice dynamics, Phys. Rev. B 73 (15) 155114.
[23] S. Baroni, S. Gironcoli, A.D. Corso, P. Gianozzi, Phonons and related crystal properties from density-functional perturbation theory, Rev. Mod. Phys. 73 (2001) 515–562.
[24] W.G. Aulbur, L. Jönsson, J.W. Wilkins, Quasiparticle calculations in solids, Solid State Phys. 54 (2000) 1–218.
[25] X. Gonze, B. Amadon, P.-M. Anglade, J.-M. Beuken, F. Bottin, P. Boulanger, F. Bruneval, D. Caliste, R. Caracas, M. Côté, T. Deutsch, L. Genovese, Ph Ghosez, M. Giantomassi, S. Goedecker, D.R. Hamann, P. Hermet, F. Jollet, G. Jomard, S. Leroux, M. Mancini, S. Mazevet, M.J.T. Oliveira, G. Onida, Y. Pouillon, T. Rangel, G.-M. Rignanese, D. Sangalli, R. Shaltaf, M. Torrent, M.J. Verstraete, G. Zerah, J.W. Zwanziger, ABINIT: first-principles approach to material and nanosystem properties, Comput. Phys. Commun. 180 (2009) 2582–2615.
[26] X. Gonze, G.-M. Rignanese, M. Verstraete, J.-M. Beuken, Y. Pouillon, R. Caracas, F. Jollet, M. Torrent, G. Zerah, M. Mikami, P. Ghosez, M. Veithen, J.-Y. Raty, V. Olevano, F. Bruneval, L. Reining, R. Godby, G. Onida, D.R. Hamann, D.C. Allan,

A brief introduction to the ABINIT software package, Z. für Kristallogr. - Cryst. Mater. 220 (2005) 558–562.
[27] S. Lebègue, B. Arnaud, M. Alouani, P.E. Bloechl, Implementation of an all-electron GW approximation based on the projector augmented wave method without plasmon Pole approximation: application to Si, SiC, AlAs, InAs, NaH, and KH, Phys. Rev. B 67 (2003) 155208.
[28] M. Born, On the stability of crystal lattices, I, Math. Proc. Cambridge 36 (2) (1940) 160–172.
[29] M. Born, K. Huang, Dynamics Theory of Crystal Lattices, Oxford University Press, Oxford, UK, 1954.
[30] F. Mouhat, F.-X. Coudert, Necessary and sufficient elastic stability conditions in various crystal systems, Phys. Rev. B 90 (22) (2014) 224104.
[31] O. Madelung, U. Rössler, M. Schulz, Silicon (eds.) (Si) Young's modulus, torsion modulus, bulk modulus (various structures), in: Group IV Elements, IV-IV and III-V Compounds. Part a - Lattice Properties. Landolt-Börnstein - Group III Condensed Matter, Springer, Berlin, Heidelberg, 2001.
[32] O. Madelung, U. Rössler, M. Schulz, Silicon (eds.) Silicon (Si) elastic moduli of Si-I, in: Group IV Elements, IV-IV and III-V Compounds. Part a - Lattice Properties. Landolt-Börnstein - Group III Condensed Matter, Springer, Berlin, Heidelberg, 2001.
[33] W. Shockley, H.J. Queisser, Detailed balance limit of efficiency of p-n junction solar cells, J. Appl. Phys. 32 (1961) 510–519.
[34] S. Rühle, Tabulated values of the Shockley–Queisser limit for single junction solar cells, Sol. Energy 130 (2016) 139–147.
[35] G.L. Zhao, D. Bagayoko, Electronic structure and charge transfer in 3C- and 4H-SiC, New J. Phys. 2 (2000) 16.1–16.12.
[36] V.A. Gritsenko, Electronic structure of silicon nitride, Phys. Uspekhi 55 (5) (2012) 498–507.
[37] P.M. Sylenko, A.M. Shlapak, S.S. Petrovska, O.Y. Khyzhun, Y.M. Solonin, V. V. Atuchin, Direct nitridation synthesis and characterization of Si_3N_4 nanofibers, Res. Chem. Intermed. 41 (2015) 10037–10048.
[38] F.C. Zhang, H.W. Cui, X.X. Ruan, W.H. Zhang, Density-functional theory study on electronic structure and optical property of 6H-SiC, Mater. Res. Innov. 19 (S6) (2015) 46–49.
[39] E. Kroumova, M.I. Aroyo, J.M. Perez-Mato, A. Kirov, C. Capillas, S. Ivantchev, H. Wondraschek, Bilbao Crystallographic Server : useful databases and tools for phase-transition studies, Phase Transitions 76 (2003) 155–170.
[40] H. Richter, Z.P. Wang, L. Ley, The one phonon Raman spectrum in microcrystalline silicon, Solid State Commun. 39 (1981) 625–629.
[41] C.J. Wen, R.A. Huggins, Chemical diffusion in intermediate phases in the lithium-silicon system, J. Solid State Chem. 37 (3) (1981) 271–278.
[42] M.N. Obrovac, L. Christensen, Structural changes in silicon anodes during lithium insertion/extraction, Electrochem Solid St 7 (5) (2004) A93–A96.
[43] J. Li, J.R. Dahn, An in situ X-ray diffraction study of the reaction of Li with crystalline Si, J. Electrochem. Soc. 154 (3) (2007) A156–A161.
[44] V.L. Chevrier, J.W. Zwanziger, J.R. Dahn, First principles study of Li–Si crystalline phases: charge transfer, electronic structure, and lattice vibrations, J. Alloy. Comp. 496 (2010) 25–36.